Applied Surface Science 258 (2012) 7154–7160

Contents lists available at SciVerse ScienceDirect

Applied Surface Science

journal homepage: www.elsevier.com/locate/apsusc

Insight into the adsorption and dissociation of CH_4 on Pt($h\,k\,l$) surfaces: A theoretical study

Riguang Zhang[a,*], Luzhi Song[a], Yuhan Wang[b]

[a] Key Laboratory of Coal Science and Technology of Ministry of Education and Shanxi Province, Taiyuan University of Technology, Taiyuan 030024, Shanxi, China
[b] School of Chemical Engineering and Environment, Beijing Institute of Technology, Beijing 100081, China

ARTICLE INFO

Article history:
Received 16 January 2012
Received in revised form 3 April 2012
Accepted 3 April 2012
Available online 10 April 2012

Keywords:
CH_4
Dissociation
Pt($h\,k\,l$) surface
Density functional theory

ABSTRACT

A density functional theory slab calculations of CH_4 dissociation on Pt($h\,k\,l$) surfaces have been systematically presented. On the basis of the energetic analysis, the favorable adsorption sites and stable configurations of CH_x(x = 0–4) and H species on Pt(1 1 1), Pt(1 1 0) and Pt(1 0 0) surfaces are first obtained, respectively. Afterwards, the most stable configurations of coadsorbed CH_x/H(x = 0–3) are located. Further, the kinetic and thermodynamical results of CH_4 dissociation on Pt($h\,k\,l$) surface suggest that CH is the most abundant CH_x species. Our results mean that Pt catalyst can resist the carbon deposition in the CH_4 dissociation, which can give a microscopic reason that why Pt catalyst can lead to lower carbon deposition and show a high activity in the reaction related to CH_4.

1. Introduction

CH_4, as one of the most important chemicals, has been widely used in chemical synthesis, hydrogen production, and energy production [1]. As the principal chemical process such as CH_4—CO_2 reforming reaction [2–10] and acetic acid synthesis via a two stepwise CH_4—CO_2 reaction [11,12], the dissociation of CH_4 on the transition metal surface has attracted great interest from both experimental [11–15] and theoretical studies [16–31] in recent years. It is generally believed that the rate-determining step for many of these heterogeneous processes is the dissociation of CH_4 on the transition metal surface [14]. For the dissociation of CH_4, it is well known that the best catalysts are the group VIII metals Ru, Rh, Pt and Ir etc., especially, the 4d and 5d group VIII metals are the most suitable catalysts, such as Pt catalyst. Moussounda et al. [28] have studied the adsorption of H, CH_3 and CH_4 on Pt(1 0 0) surface. Petersen et al. [32] have investigated the adsorption of CH_4 dissociation intermediates, CH_x (x = 0–3), on Pt{1 1 0}(1 × 2) using density functional theory (DFT) method, and they found that CH_3 preferentially occupies the ridge atop site; CH_2 is at the ridge bridge site; CH, is at the 3-fold fcc site on the {1 1 1} microfacet; carbon, the pseudosubsurface 4-fold site at the bottom of the trough. Meanwhile, for other chemical substances, it has been widely studied and applied on Pt catalyst. Medlin and Allendorf [33] have studied the adsorption of acetylene and hydrogen on the (1 1 1) surface of Pd, Pt, Ni, and Rh. Anghel et al. [34,35] have studied the sequential dissociation of ethane or C_2H_x on Pt(1 1 0) surface using DFT method.

Nowadays, experimental researchers have investigated the dissociative sticking coefficient for CH_4 on Pt(1 1 1) surface as a function of both gas temperature (T_g) and surface temperature (T_s) using effusive molecular beam and angle-integrated ambient gas dosing methods [15]. Ukraintsev and Harrison [13] have studied the statistical model of activated dissociative adsorption using microcanonical, unimolecular rate theory. Luntz and Bethune [14] have detailed molecular beam measurements of the dissociative chemisorption probability for CH_4 on Pt(1 1 1) surface. On the other hand, theoretical calculations about CH_4 dissociation on group VIII metal surface have been extensively investigated by using DFT method. However, most of them are focused on the Co [7,24,31], Ni [2–6,8,20], Ru [16,17,25,26], Rh [19,21–23], Pd [9,18] and Ir [36] surface. For the CH_4 dissociation on Pt($h\,k\,l$) surface, only Petersen et al. [27,32] studied the dissociation of CH_4 on Pt{1 1 0}(1 × 2) surface using DFT methods. Meanwhile, other studies only involves the adsorption of CH_x on Pt surface [28,37–42] and the dissociation of CH_4 on Pt(1 1 1) surface [29,30]. To the best of our knowledge, it is a pity that few theoretical studies are systematically carried out to investigate and compare the dissociation of CH_4 on Pt(1 1 1), Pt(1 1 0) and Pt(1 0 0) surfaces, respectively. Recently, theoretical computation methods have become a powerful research tool for understanding the chemical reactions in the microscopic view. For example, methods based on quantum chemical theory can well

* Corresponding author at: No. 79 Yingze West Street, Taiyuan 030024, China. Tel.: +86 351 6018239; fax: +86 351 6041237l.
E-mail addresses: zhangriguang@tyut.edu.cn, zhangriguang1981@163.com (R. Zhang).

0169-4332/$ – see front matter © 2012 Elsevier B.V. All rights reserved.
http://dx.doi.org/10.1016/j.apsusc.2012.04.020

provide information at atomic/molecular level. In particular, DFT method can provide the accurate energetic, geometries and reaction barriers [31].

Therefore, in this study, we present a systematic study about the successive dissociation of CH_4 on Pt(1 1 1), Pt(1 1 0) and Pt(1 0 0) surfaces using DFT method, which may be of interest to researchers attempting to illustrate the catalytic mechanism involving in CH_4 reaction on Pt catalyst. This paper is organized as follows: in Section 2, we provide the detailed models and computational methods, in Section 3, we present the relative investigations of CH_x(x = 0–4) and H adsorption on Pt($h\,k\,l$) surface; then, the coadsorbed configurations of CH_x/H(x = 0–3) on Pt($h\,k\,l$) surface; finally, we discuss the dissociation mechanism of CH_4 on Pt($h\,k\,l$) surface.

2. Methods and models

Density functional theory (DFT) periodic calculations are carried out with the Cambridge Sequential Total Energy Package (CASTEP) [43,44]. In this code, the Kohn–Sham equations are solved using the generalized gradient approximation (GGA) as proposed by Perdew–Wang-91 (PW91) [45,46] to describe all exchange and correlation effects. We use the Vanderbilt-type ultrasoft pseudopotentials [47], with plane wave basis sets with a cutoff energy of 280 eV [33,48]. Meanwhile, our test results with a cutoff energy of 340 eV indicate that the error between 280 eV and 340 eV is negligible. The k-points meshes are set to $4 \times 4 \times 1$ for Pt(1 1 1), $2 \times 4 \times 1$ for Pt(1 1 0) and $4 \times 4 \times 1$ for Pt(1 0 0) surface. The convergence criteria for structure optimization and energy calculation are set to 2.0×10^{-6} eV/atom, 2.0×10^{-5} eV/atom, 0.05 eV/Å and 2.0×10^{-3} Å for the tolerance of SCF, energy, maximum force, and maximum displacement, respectively. Since metal Pt is not a magnetic material, spin polarization on Pt has not been considered. Transition states (TS) are located by using the complete LST/QST method [49], the linear synchronous transit (LST) maximization is performed followed by an energy minimization in directions conjugate to the reaction pathway. The TS approximation obtained in that way is used to perform quadratic synchronous transit (QST) maximization. From that point, another conjugate gradient minimization is performed. The cycle is repeated until a stationary point is located. In addition, for the validation of transition state involving the reaction, since CASTEP program cannot obtain the frequency information, Dmol^3 program is employed to calculate the frequency of transition state with the same calculation methods, and TS confirmation is performed on every transition state to confirm that they lead to the desired reactants and products.

The Pt($h\,k\,l$) surface are modeled using a four layers Pt slab with the bottom one layer fixed at their positions in the bulk and the uppermost three layers relax. Periodic boundary conditions are used to model an extended surface. The vacuum region separating the slabs in the direction perpendicular to the surface is set to 10 Å. A $p(2 \times 2)$ supercell is used in the calculation, as shown in Fig. 1. For Pt(1 1 1) surface, there are four adsorption sites: top (T), bridge (B), fcc, hcp; for Pt(1 1 0) surface, top (T), short bridge (SB), long bridge (LB), hollow (H); for Pt(1 0 0) surface, top (T), bridge (B), hollow (H). In addition, a $p(2 \times 3)$ surface supercell has also been considered to obtain the size effect of surface on calculation results, which suggest that a $p(2 \times 2)$ supercell is large enough to neglect the lateral interactions of the adsorbate.

The adsorption energy is defined as follows:

$$E_{ads} = E_{adsorbate} + E_{slab} - E_{adsorbate+slab}$$

where $E_{adsorbate+slab}$ is the total energy of the slab together with the adsorbate, $E_{adsorbate}$ is the total energy of the free adsorbate, and E_{slab} is the total energy of the bare slab. According to this definition, positive energy values correspond to an energetically favorable adsorption.

3. Results and discussion

3.1. Calculation of bulk Pt and CH_4 molecule

In order to verify the reliability of the selected calculation methods, we first calculated the lattice constant of bulk Pt (4.008 Å), which is close to the experimental value of 3.924 Å [50], as well as with other similar GGA results [28,41]. Then, the next test is to obtain the bond length and bond angle of CH_4, both are $r_{(C-H)}$ = 1.096 Å and $\theta_{(H-C-H)}$ = 109.5°, respectively, which agrees with the experimental values of 1.096 Å and 109.4° [51]. Such results obtained in these tests are in agreement with the experimental values.

3.2. Single adsorption of CH_x(x = 0–4) and H species on Pt($h\,k\,l$) surface

Before we investigate the mechanism of CH_4 dissociation on Pt($h\,k\,l$) surface, it is necessary to know the individual bonding natures of different species adsorbed on Pt($h\,k\,l$) surface. Thus, we first investigate the most stable configurations of H and CH_x(x = 0–4) species on Pt($h\,k\,l$) surface, in which different adsorption sites on Pt($h\,k\,l$) surface are considered. Then, we can obtain the most stable configurations of coadsorbed CH_x/H(x = 0–3) on Pt($h\,k\,l$) surface. Further, we discuss the mechanism of CH_4 dissociation to the final products C and H, in which every elementary reaction has been analyzed in detailed.

3.2.1. CH_x and H adsorbed on Pt(1 1 1)

For CH_4, the adsorption on transition metal surfaces is generally classified as a process of physisorption where the attractive interaction arises from the van der Waals force. Four stable structures are found, CH_4(T), CH_4(B), CH_4(fcc) and CH_4(hcp), the corresponding adsorption energies are 3.8, 3.0, 3.5 and 3.4 kJ mol^{-1}, respectively. The most stable configuration is adsorption at the top site, as shown in Fig. 2(a). We can see that the Pt—H distance is 2.229 Å, and one C—H bond length is (1.114 Å) larger than that (1.096 Å) of free CH_4. Meanwhile, our calculated adsorption energy is close to that obtained in previous theoretical studies of CH_4 adsorption on Pt(1 1 1) surface [29,30]. Dianat et al. [52] obtained an adsorption energy of 7.7 kJ mol^{-1} for CH_4 adsorption on pure metallic Pt(1 1 1) surface from their DFT slab calculations.

For CH_3, the initial structure at the bridge, fcc and hcp site are all optimized into that at the top site. Thus, only one stable structure at the top site can been obtained, the adsorption energy is 264.3 kJ mol^{-1} for CH_3 (T), as shown in Fig. 2(b), which is consistent with the earlier calculations on Pt(1 1 1) [53]. The C—Pt bond lengths are 2.077 Å, and all C—H bond lengths are 1.096 Å.

For CH_2, at the top, fcc and hcp sites, the corresponding adsorption energies are 376.6, 439.9 and 425.7 kJ mol^{-1}, respectively. The most stable adsorption site is bridge site (see Fig. 2(c)), and the adsorption energy is 465.3 kJ mol^{-1}. The C—H bond lengths are 1.097 and 1.099 Å, respectively, the angle of H—C—H is 112.7° for the bridge adsorption mode, the C—Pt bond lengths are 2.068 and 2.069 Å, respectively.

For CH, the initial structures at the top and bridge sites are all optimized into that at the fcc site, respectively. CH interacts with three Pt atoms forming three Pt—C bonds at the fcc site, which is the most stable configuration (see Fig. 2(d)). The C—H bond length is shorten to 1.096 Å from that of free CH (1.136 Å), and the C—Pt bond lengths are 2.020, 2.023 and 2.021 Å at the fcc site, the adsorption

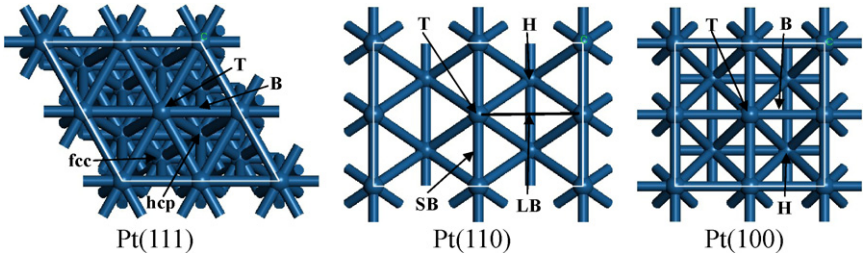

Fig. 1. Top view of Pt($h\,k\,l$) surface. Top site-T; bridge site-B; hollow site-H; short bridge-SB; long bridge-LB.

energy is 697.3 kJ mol^{-1}. At the hcp site, the adsorption energy is 690.2 kJ mol^{-1}.

For C, four stable structures are obtained. At the fcc site, C interacting with three Pt atoms is the most stable configuration (see Fig. 2(e)). The adsorption energy is 791.9 kJ mol^{-1}. C—Pt bond lengths are 1.943, 1.945 and 1.946 Å. At the top, bridge and hcp sites, the corresponding adsorption energies are 575.9, 712.3 and 785.2 kJ mol^{-1}, respectively.

For H, three stable structures are found; the initial structure at the bridge site is converted into that at the fcc site. At the top, fcc and hcp sites, the corresponding adsorption energies are 373.7, 380.3 and 380.1 kJ mol^{-1}, respectively, which suggests that H prefers to adsorb at the three-fold site, as shown in Fig. 2(f), the C—Pt bond lengths are 1.875, 1.878 and 1.878 Å.

Based on the above results, we can conclude that CH_4 adsorbed at four sites of Pt(1 1 1) surface is typical of physisorption. However, CH_x(x = 0–3) and H species adsorbed on Pt(1 1 1) surface is a strong chemisorption, in which CH_3 prefers to adsorb at the top site, CH_2 prefers to adsorb at the bridge site, CH, C and H prefer to adsorb at the fcc sites. A similar structure was also obtained by Zhu et al. [41] for CH_x adsorption on Pt(1 1 1) surface, and a related structure was determined by Chen and Vlachos [29], as well as Viñes et al. [30] in their calculations of CH_x adsorption on Pt(1 1 1) surface.

3.2.2. CH_x and H adsorbed on Pt(1 1 0)

The most stable adsorption configuration of CH_x(x = 0–3) and H species on Pt(1 1 0) surface with the key geometrical parameters are presented in Fig. 3.

For CH_4, CH_4 adsorbed at the top site is the most stable configuration (see Fig. 3(a)), in which CH_4 molecule is not distorted. The Pt—H distance is 2.090 Å, and the adsorption energy is 44.5 kJ mol^{-1}. CH_3 prefers to the top site with the C—Pt bond length of 2.062 Å, as shown in Fig. 3(b), and the adsorption energy is 322.0 kJ mol^{-1}. CH_2 adsorbs at the SB site with the C—Pt bond lengths of 2.050 and 2.051 Å, respectively, as seen in Fig. 3(c). The corresponding adsorption energy is 560.5 kJ mol^{-1}. CH prefers to the three-hold hollow site with the C—Pt bond lengths of 2.072, 1.996 and 1.996 Å, as presented in Fig. 3(d), the adsorption energy is 736.8 kJ mol^{-1}. For C atom, C prefers to adsorb at the LB site with the C—Pt bond lengths of 1.965 and 1.967 Å, respectively, (see Fig. 3(e)), the corresponding adsorption energy is 873.0 kJ mol^{-1}. Finally, H adsorbed at the SB site is the most stable configuration with H—Pt bond lengths of 1.767 and 1.768 Å, respectively, as shown in Fig. 3(f), the corresponding adsorption energy is 426.3 kJ mol^{-1}. Our calculated results about the adsorption of CH_x on Pt(1 1 0) surface are in good agreement with the studies by Moussounda et al. [28], which show the chemisorption of CH_x on Pt{1 1 0}(1 × 2) surface.

3.2.3. CH_x and H adsorbed on Pt(1 0 0)

CH_4 adsorbed at the top site (see Fig. 4(a)) is the most stable configuration with the adsorption energy of 3.8 kJ mol^{-1}, and CH_4 molecule is still not distorted. CH_3 prefers to adsorb at the top site with the C—Pt bond length of 2.074 Å, as shown in Fig. 4(b), the corresponding adsorption energy is 266.9 kJ mol^{-1}. CH_2 prefers to adsorb at the bridge site with the C—H bond lengths of 1.098 and 1.099 Å, respectively, as well as the angle of H—C—H of 113.6°, as seen in Fig. 4(c), the adsorption energy is 507.0 kJ mol^{-1}. CH prefers to adsorb at the hollow site, as presented in Fig. 4(d), the adsorption energy is 716.4 kJ mol^{-1}. The C—H bond length is 1.104 Å, and all C—Pt bond lengths are 2.156 Å. C adsorbed at the hollow site is the most stable configuration with the adsorption energy of 864.2 kJ mol^{-1} (see Fig. 4(e)), all the C—Pt bond lengths are 2.052 Å.

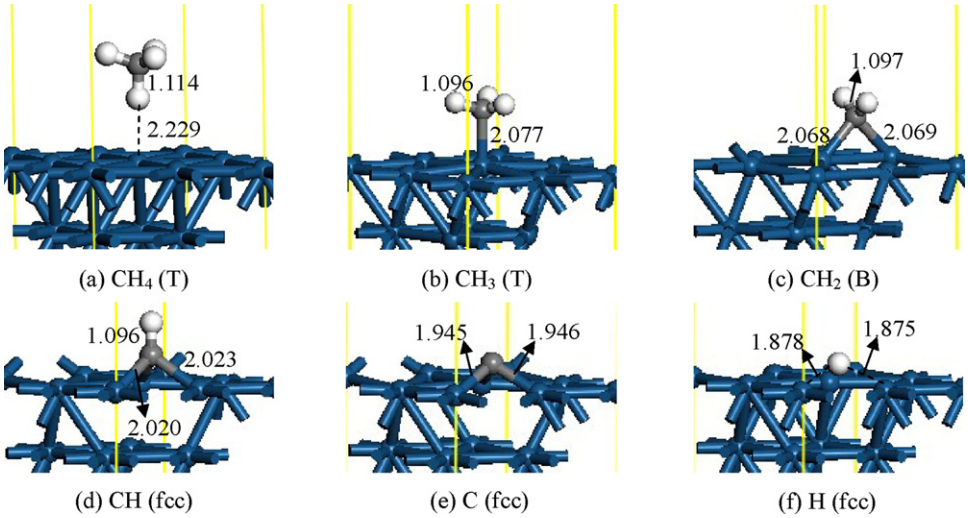

Fig. 2. The most stable configuration of CH_x and H adsorb on Pt(1 1 1) surface (unit: bond length in Å). The C, H and Pt atoms are shown in the grey, white, and dark-blue colors, respectively. (For interpretation of the references to color in this figure legend, the reader is referred to the web version of the article.)

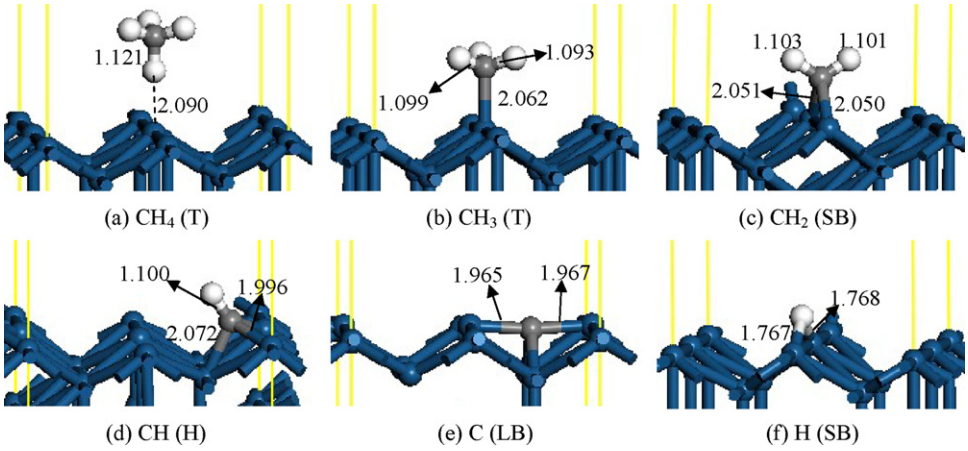

Fig. 3. The most stable configuration of CH_x and H adsorb on Pt(1 1 0) surface.

For H atom, H adsorbed at the bridge site is the most stable configuration with the adsorption energy of 391.6 kJ mol^{-1}, as shown in Fig. 4(f), all H—Pt bond lengths are 1.767 Å.

Above results about the single adsorption of CH_x(x = 0–4) and H species on Pt($h\,k\,l$) surface show that although the discrepancies among the various studies exist in the precise values for the adsorption energies, all these studies can conclude the general trend in the adsorption energies: $CH_4 < CH_3 < H < CH_2 < CH < C$. Our calculated results agree with the previous reported results [29,30,32,38,41].

3.3. The coadsorbed CH_x/H(x = 0–3) on Pt($h\,k\,l$) surface

In order to map out the reaction mechanism of CH_4 sequential dissociation on Pd(1 1 1) surface, we need to establish the coadsorbed configurations of CH_x(x = 0–3) and H on Pd(1 1 1) surface.

The coadsorbed energy of CH_x/H on Pt($h\,k\,l$) surface can be defined as follows:

$$E_{\text{coads}} = E(\text{CH}_x) + E(\text{H}) + E(\text{Pt slab}) - E((\text{CH}_x/\text{H}) + \text{Pt slab})$$

where $E(CH_x)$, E(H), E(Pt slab) and $E((CH_x/H)$ + Pt slab) are the total energy for the free CH_x species and hydrogen atom, Pt slab with a (2×2) supercell and the coadsorbed (CH_x/H) + Pt slab systems, respectively.

For the most stable coadsorbed configurations of CH_x/H species on Pt($h\,k\,l$) surface, we consider that CH_x(x = 0–3) and H are placed at their adjacent and the most stable adsorption sites. For example, for the most stable coadsorbed configuration of CH_3/H on Pt(1 1 1) surface, it has been pointed out that the CH_3 at the top site is the most stable configuration, and H placed at the fcc site is the most stable configuration. As a result, in the initial coadsorbed configuration of CH_3/H on Pt(1 1 1) surface, CH_3 and H are placed at the adjacent top and fcc site, respectively. The optimized stable coadsorbed configuration is shown in Fig. 5(a), and the coadsorbed energy is 635.9 kJ mol^{-1}, in which the distance of H—CH_3 is 3.595 Å. Afterwards, Fig. 5(b) gives the stable coadsorbed configuration of CH_2/H on Pt(1 1 1) surface, in which CH_2 and H are located at the adjacent bridge and fcc sites, respectively, and the coadsorbed energy is 832.4 kJ mol^{-1}, the distance of H—CH_2 is 3.034 Å. Further, the stable coadsorbed configuration of CH/H is presented in Fig. 5(c), in which CH and H site are located at the adjacent fcc and top sites, respectively, and the coadsorbed energy is 1054.8 kJ mol^{-1}, the distance of H—CH is 3.223 Å. Finally, the stable coadsorbed configuration of C/H are shown in Fig. 5(d), in which C and H are adsorbed at the adjacent fcc and fcc sites, respectively, and the coadsorbed energy is 1147.8 kJ mol^{-1}, the distance between H and C is 2.840 Å. As a result, the optimized stable configurations of coadsorbed CH_x/H system with key structural parameters on Pt($h\,k\,l$) surface are presented in Figs. 5–7, they are denoted as CH_x/H, the corresponding

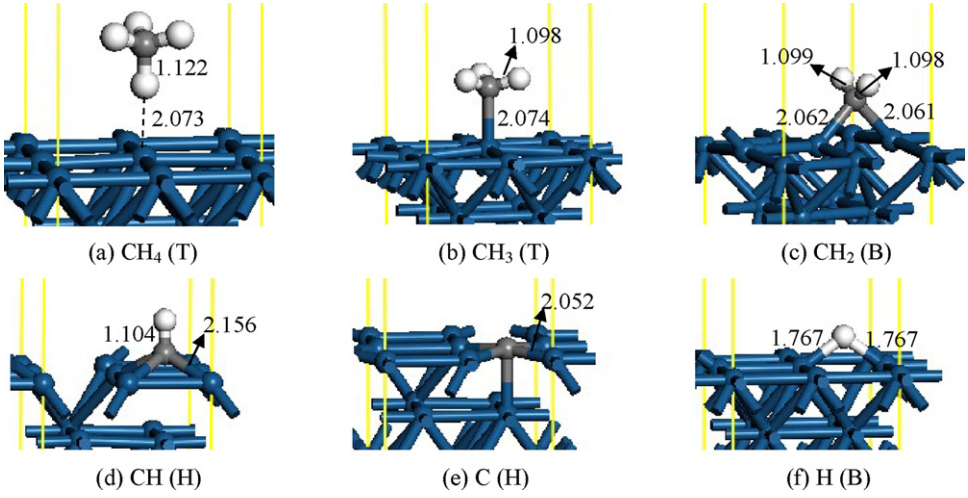

Fig. 4. The most stable configuration of CH_x and H adsorb on Pt(1 0 0) surface.

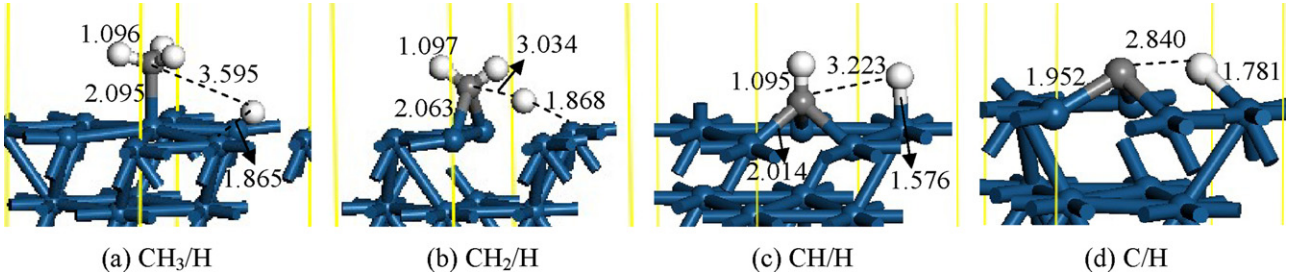

Fig. 5. The optimized stable coadsorbed configurations of CH_x/H on Pt(1 1 1) surface.

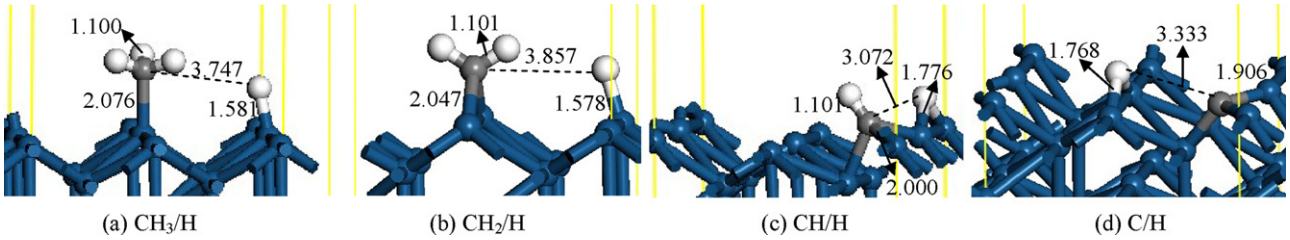

Fig. 6. The optimized stable coadsorbed configurations of CH_x/H on Pt(1 1 0) surface.

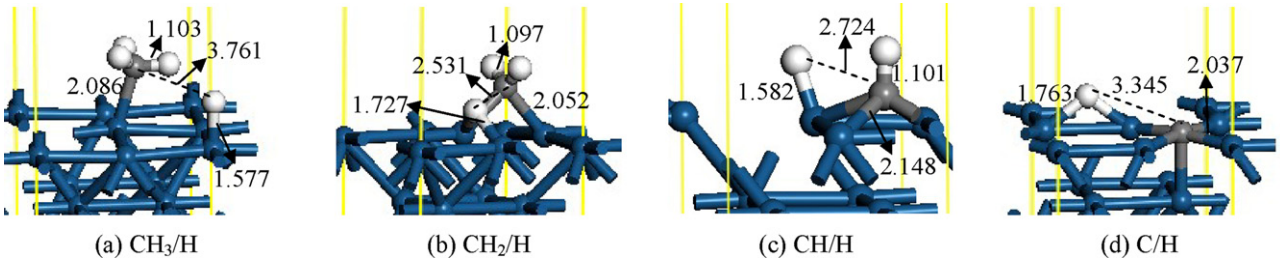

Fig. 7. The optimized stable coadsorbed configurations of CH_x/H on Pt(1 0 0) surface.

coadsorbed energies and the adsorption sites are listed in Table 1.

3.4. CH_4 sequential dissociation on Pt(h k l) surface

In Section 3.3, we have obtained the most stable coadsorbed configuration of CH_x/H(x = 0–3) species: CH_3/H, CH_2/H, CH/H, C/H, then the elementary step of CH_4 sequential dissociation on Pt(*h k l*) surface can been discussed. CH_4 dissociation on metal surfaces has four steps as follows: the first step is CH_4 dissociation into CH_3/H with the transition state TS1, the second step is CH_3 dissociation into CH_2/H with TS2, the third step is CH_2 dissociation into CH/H with TS3, and the fourth step is CH dissociation into C/H with TS4. As a result, for the first step of CH_4 dissociation into CH_3/H, the most stable configuration of CH_4 is chosen to be the initial state, and the final state consists of the stable coadsorbed CH_3/H configuration. The dissociation of other CH_x(x = 1–3) species is similar to that of CH_4 dissociation. The corresponding transition state structures for CH_4 dissociation on Pt(1 1 1), Pt(1 1 0) and Pt(1 0 0) surfaces are shown in Fig. 8(a)–(c), respectively.

In this study, the dissociation energy barriers and reaction energies of the most favorable step for CH_4 dissociation on Pt(1 1 1), Pt(1 1 0) and Pt(1 0 0) surfaces are obtained, and the corresponding thermodynamic and kinetic schemes of CH_4 dissociation on Pt(*h k l*) surface are given in Fig. 9, which illustrates the energy change for the whole process of CH_4 dissociation from CH_4 to C.

As shown in Fig. 9, the reaction energies of CH_4 complete dissociation are 93.9, −28.4 and 9.0 kJ mol^{-1} on Pt(1 1 1), Pt(1 1 0) and Pt(1 0 0) surfaces, respectively. In gas phase, CH_4 sequential dissociation is endothermic, and the computed reaction energies are 457.3, 479.5, 479.5 and 350.2 kJ mol^{-1} for each step, which means that a total of 1766.5 kJ mol^{-1} is needed for the complete dissociation [20]. Comparatively, the reaction is advantaged on Pt surface thermodynamically.

On the basis of thermodynamic reaction energies, we can see that on Pt(1 1 1) surface, CH is the most abundant CH_x species, followed by CH_3 and CH_2. However, only very small quantity of surface

Table 1
The coadsorbed energies (kJ mol^{-1}) and the adsorption sites in the stable coadsorbed configuration of CH_x/H on Pt(*h k l*) surface.

	CH_3/H		CH_2/H		CH/H		C/H	
	Model	E_{coads}	Model	E_{coads}	Model	E_{coads}	Model	E_{coads}
Pt(1 1 1)	T-fcc[a]	635.9	B-fcc	832.4	fcc-T	1054.8	fcc-fcc	1147.8
Pt(1 1 0)	T-T	706.4	SB-LB	934.4	H-SB	1116.7	H-SB	1260.8
Pt(1 0 0)	T-T	636.3	B-B	879.7	H-T	1095.2	H-B	1237.9

[a] T-fcc denotes that on Pt(1 1 1) surface, CH_3 and H are adsorbed at the adjacent top site and fcc site in the stable coadsorbed configuration of CH_3/H. Other models are the same meanings.

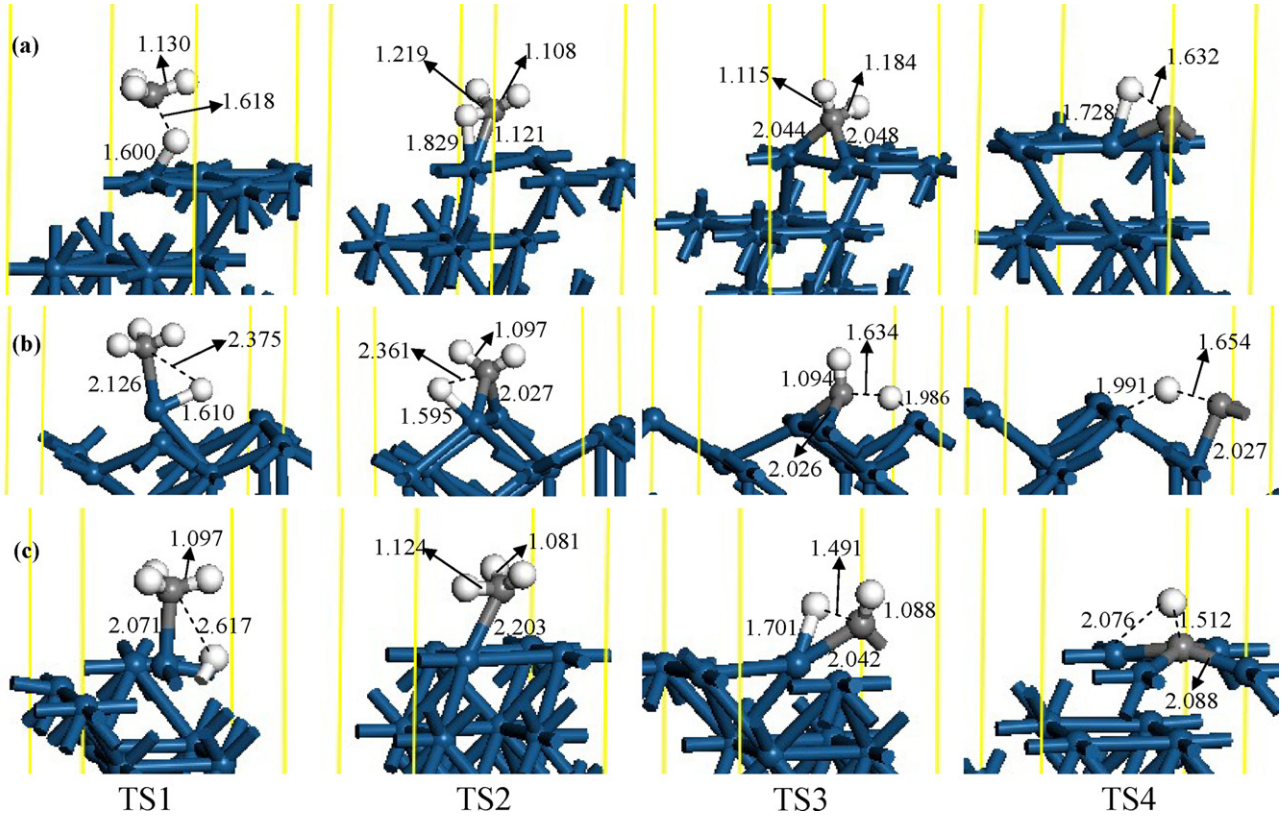

Fig. 8. The transition state structures for CH_4 dissociation on (a) Pt(1 1 1), (b) Pt(1 1 0) and (c) Pt(1 0 0) surfaces.

carbon exists because of its high energy. In general, CH_4 dissociation on Pt(1 1 1) is endothermic. On Pt(1 1 0) surface, both CH_2 and CH are the most abundant CH_x species, and the other species are higher in energy, and this agrees with the CH_x stability sequence obtained by Petersen et al. [32]. On the whole, the dissociation of CH_4 on Pt(1 1 0) surface is exothermic, indicating the preference of dissociation process on Pt(1 1 0) surface. On Pt(1 0 0) surface, CH is the most abundant CH_x species for CH_4 dissociation, followed by CH_2 and CH_3. Therefore, CH_4 dissociation on Pt(1 0 0) and Pt(1 1 1) surfaces is endothermic, indicating that this process on Pt(1 0 0) and Pt(1 1 1) surfaces is relatively unfavorable in comparison with that on Pt(1 1 0) surface.

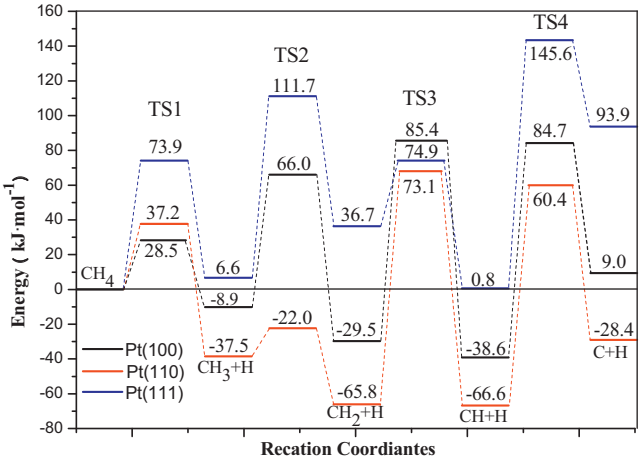

Fig. 9. The energy profiles of the dissociation from CH_4 to C on Pt(*h k l*) surface.

On the other hand, it is to note that the conclusions in above results are only based on thermodynamics, and they are limited regarding kinetics. As a result, we analyze the CH_4 dissociation based on kinetics. Similarly, as shown in Fig. 9, on Pt(1 1 1) surface, the first step, CH_4 dissociates into CH_3/H, needs to overcome an activation barrier of 73.9 kJ mol^{-1}, and that of back reaction is 67.3 kJ mol^{-1}. In the second step, the activation barrier of CH_3 dissociates into CH_2/H is 105.1 kJ mol^{-1}, and that of its back reaction barrier is 75.0 kJ mol^{-1}. In the third step, CH_2 dissociates into CH/H needs to overcome an activation barrier of 38.2 kJ mol^{-1}, and that of its back reaction barrier is 74.1 kJ mol^{-1}. In the last step, CH dissociates into C/H needs to overcome a very large activation barrier of 144.8 kJ mol^{-1}, and its back reaction barrier is 51.7 kJ mol^{-1}, which show that the last step of CH_4 dissociation is a strong endothermic process. Meanwhile, CH_2 can be easily dissociated into CH with a low barriers 38.2 kJ mol^{-1}, and CH can be hydrogenated to CH_3 with a relatively high barriers of 75.0 kJ mol^{-1}, which indicates that among all the dissociation products (CH_3, CH_2, CH and C), CH_2 is expected to be the least stable. Consequently, the lifetime of CH_2 is likely to be short and its concentration must be quite low under real conditions. Further, the high barrier and the strong endothermicity of CH dissociation on Pt(1 1 1) surface indicate that this reaction is unfavorable both kinetically and thermodynamically. Our results are in good agreement with those obtained by Chen and Vlachos [29] and Viñes et al. [30]. Therefore, CH is the most abundant species on Pt(1 1 1) surface.

On Pt(1 1 0) surface, in the first step, CH_4 dissociates into CH_3/H, which needs to overcome an activation barrier of 37.2 kJ mol^{-1}, and that of back reaction is 74.7 kJ mol^{-1}. In the second step, the activation barrier of CH_3 dissociates into CH_2/H is 15.5 kJ mol^{-1}, and that of its back reaction is 43.8 kJ mol^{-1}. In the third step, CH_2 dissociates into CH/H needs to overcome an activation barriers of 138.9 kJ mol^{-1}, and that of hydrogenation of CH_2 to CH_3 is

139.7 kJ mol^{-1}. In the fourth step, CH dissociates into C/H needs to overcome an activation barrier of 127.0 kJ mol^{-1}, and its back reaction barrier is 88.8 kJ mol^{-1}. Above results show that CH_3 dissociates into CH_2/H is the most favored step kinetically, followed by CH_4, CH and CH_2, however, the differences of activation barrier for CH_2 and CH dissociation are small, CH dissociation is a strong endothermic process, and CH_2 dissociation is a slightly exothermic process. Thus, we think that CH is the most abundant species on Pt(1 1 0) surface, these results are similar with those obtained by Petersen et al. [32].

On Pt(1 0 0) surface, CH_4 dissociating into CH_3/H needs to overcome an activation barrier of 28.5 kJ mol^{-1}, and that of back reaction is 37.4 kJ mol^{-1}. Then, the activation barrier of CH_3 dissociating into CH_2/H is 74.9 kJ mol^{-1}, and that of its back reaction barrier is 95.5 kJ mol^{-1}. In the third step, CH_2 dissociates into CH/H needs to overcome an activation barrier of 114.9 kJ mol^{-1}, and that of hydrogenation of CH_2 to CH_3 is 124.0 kJ mol^{-1}. In the fourth step, CH dissociates into C/H needs to overcome a barrier of 123.3 kJ mol^{-1}, and its back reaction barrier is 75.7 kJ mol^{-1}, indicating that CH dissociation is a strong endothermic process. Therefore, the high barriers and the strong endothermicity of CH dissociation mean that CH dissociation on Pt(1 0 0) surface is also unfavorable both kinetically and thermodynamically, as a result, CH is also the most abundant species on Pt(1 0 0) surface.

According to above thermodynamical and kinetic results, we can obtain that on Pt(1 1 1), Pt(1 1 0) and Pt(1 0 0) surfaces, CH is the most abundant CH_x species of CH_4 dissociation on Pt catalyst. Therefore, surface carbon is hard to form on Pt catalyst, which means the decrease possibility for the formation of carbon monoxide and carbon deposition in CH_4 reforming systems. Further, above results also show that in the reaction related to CH_4 reaction, Pt catalyst can well resist carbon deposition.

4. Conclusions

The dissociation of CH_4 on Pt($h\,k\,l$) surface has been investigated by using density functional theory slab calculation. On the basis of energetic analysis, CH_4 is favored to dissociate into CH_3, then transformed to CH_2 and CH by sequential dissociation. On Pt(1 1 1) surface, CH_3 prefer to adsorb at the top sites, other CH_x species and H prefer to adsorb at the three-fold sites. On Pt(1 1 0) surface, the preferred sites are different, short bridge site for CH_2 and H, long bridge site for C, top site for CH_3, hollow site for H. On Pt(1 0 0) surface, the hollow site is preferred for CH and C, bridge site for CH_2 and H, CH_3 prefers to adsorb at the top site. The adsorption energies of CH_x(x = 0–4) and H adsorption show the order: $CH_4 < CH_3 < H < CH_2 < CH < C$. Meanwhile, the kinetic and thermodynamic results of CH_4 dissociation show that on Pt(1 1 1), Pt(1 1 0) and Pt(1 0 0) surfaces, CH is the most abundant CH_x species. Therefore, our results can give a microscopic understanding that why Pt catalyst can lead to lower carbon deposition and show a high activity in the reaction related to CH_4.

Acknowledgment

The authors gratefully acknowledge the financial support of this study by the National Natural Science Foundation of China (grant no. 20906066, 20976115 and 21103120)

References

[1] L. Xiao, L.C. Wang, Journal of Physical Chemistry B 111 (2007) 1657–1663.
[2] D.W. Blaylock, T. Ogura, W.H. Green, G.J.O. Beran, Journal of Physical Chemistry C 113 (2009) 4898–4908.
[3] Y.A. Zhu, D. Chen, X.G. Zhou, W.K. Yuan, Catalysis Today 148 (2009) 260–267.
[4] M.F. Haroun, P.S. Moussounda, P. Légaré, Journal of Molecular Structure (THEOCHEM) 903 (2009) 83–88.
[5] W. An, X.C. Zeng, C.H. Turner, Journal of Chemical Physics 131 (2009), 174702-1-174702-11.
[6] S.G. Wang, X.Y. Liao, J. Hu, D.B. Cao, Y.W. Li, J.G. Wang, H.J. Jiao, Surface Science 601 (2007) 1271–1284.
[7] Z.J. Zuo, W. Huang, P.D. Han, Z.H. Li, Applied Surface Science 256 (2010) 5929–5934.
[8] S.G. Wang, D.B. Cao, Y.W. Li, J.G. Wang, H.J. Jiao, Journal of Physical Chemistry B 110 (2006) 9976–9983.
[9] J.F. Paul, P. Sautet, Journal of Physical Chemistry B 102 (1998) 1578–1585.
[10] M.C.J. Bradford, M.A. Vannice, Catalysis Reviews Science and Engineering 41 (1999) 1–42.
[11] W. Huang, K.C. Xie, J.P. Wang, Z.H. Gao, L.H. Yin, Q.M. Zhu, Journal of Catalysis 201 (2001) 100–104.
[12] Y.H. Ding, W. Huang, Y.G. Wang, Fuel Processing Technology 88 (2007) 319–324.
[13] V.A. Ukraintsev, I. Harrison, Journal of Chemical Physics 101 (1994) 1564–1581.
[14] A.C. Luntz, D.S. Bethune, Journal of Chemical Physics 90 (1989) 1274–1280.
[15] K.M. DeWitt, L. Valadez, H.L. Abbott, K.W. Kolasinski, I. Harrison, Journal of Physical Chemistry B 110 (2006) 6705–6713.
[16] I.M. Ciobîcă, F. Frechard, R.A. van Santen, A.W. Kleyn, J.P.J. Hafner, Journal of Physical Chemistry B 104 (2000) 3364–3369.
[17] H.L. Abbott, I. Harrison, Journal of Catalysis 254 (2008) 27–38.
[18] C.J. Zhang, P. Hu, Journal of Chemical Physics 116 (2002) 322–327.
[19] B.S. Bunnik, G.J. Kramer, Journal of Catalysis 242 (2006) 309–318.
[20] S.G. Wang, D.B. Cao, Y.W. Li, J.G. Wang, H.J. Jiao, Surface Science 600 (2006) 3226–3234.
[21] A. Kokalj, N. Bonini, C. Sbraccia, S. de Gironcoli, S. Baroni, Journal of the American Chemical Society 126 (2004) 16732–16733.
[22] M.S. Liao, Q.E. Zhang, Journal of Molecular Catalysis A: Chemical 136 (1998) 185–194.
[23] C.T. Au, C.F. Ng, M.S. Liao, Journal of Catalysis 185 (1999) 12–22.
[24] H. Burghgraef, A.P.J. Jansen, R.A. van Santen, Surface Science 324 (1995) 345–356.
[25] I.M. Ciobîcă, R.A. van Santen, Journal of Physical Chemistry B 106 (2002) 6200–6205.
[26] I.M. Ciobîcă, F. Frechard, R.A. van Santen, A.W. Kleyn, J.P.J. Hafner, Chemical Physics Letters 311 (1999) 185–192.
[27] M.A. Petersen, S.J. Jenkins, D.A. King, The Journal of Physical Chemistry B 108 (2004) 5920–5929.
[28] P.S. Moussounda, M.F. Haroun, G. Rakotovelo, P. Légaré, Surface Science 601 (2007) 3697–3701.
[29] Y. Chen, D.G. Vlachos, Journal of Physical Chemistry C 114 (2010) 4973–4982.
[30] F. Viñes, Y. Lykhach, T. Staudt, M.P.A. Lorenz, C. Papp, H.P. Steinrück, J. Libuda, K.M. Neyman, A. Görling, Chemistry: A European Journal 16 (2010) 6530–6539.
[31] H.Y. Liu, R.G. Zhang, R.X. Yan, B.J. Wang, K.C. Xie, Applied Surface Science 257 (2011) 8955–8964.
[32] M.A. Petersen, S.J. Jenkins, D.A. King, Journal of Physical Chemistry B 108 (2004) 5909–5919.
[33] J.W. Medlin, M.D. Allendorf, Journal of Physical Chemistry B 107 (2003) 217–223.
[34] A.T. Anghel, D.J. Wales, S.J. Jenkins, D.A. King, Chemical Physics Letters 413 (2005) 289–293.
[35] A.T. Anghel, D.J. Wales, S.J. Jenkins, D.A. King, Journal of Chemical Physics 126 (2007), 044710-1-044710-13.
[36] G. Henkelman, H. Jónnson, Physical Review Letters 86 (2001) 664–667.
[37] G. Papoian, J.K. Nørskov, R. Hoffmann, Journal of the American Chemical Society 122 (2000) 4129–4144.
[38] A.V. Zeigarnik, R.E. Valdés-Pérez, O.N. Myatkovskaya, Journal of Physical Chemistry B 104 (2000) 10578–10587.
[39] T. Jacob, W.A. Goddard, Journal of Physical Chemistry B 109 (2005) 297–311.
[40] J. Kua, W.A. Goddard, Journal of Physical Chemistry B 102 (1998) 9492–9500.
[41] H.Y. Zhu, W.Y. Guo, R.B. Jiang, L.M. Zhao, X.Q. Lu, M. Li, D.L. Fu, H.H. Shan, Langmuir 26 (2010) 12017–12025.
[42] G. Psofogiannakis, A. St-Amant, M. Ternan, Journal of Physical Chemistry B 110 (2006) 24593–24605.
[43] M.C. Payne, D.C. Allan, T.A. Arias, J.D. Joannopoulos, Reviews of Modern Physics 64 (1992) 1045–1097.
[44] V. Milman, B. Winkler, J.A. White, C.J. Pickard, M.C. Payne, E.V. Akhmatsakaya, R.H. Nobes, International Journal of Quantum Chemistry 77 (2000) 895–910.
[45] J.P. Perdew, A. Zunger, Physical Review B 23 (1981) 5048–5079.
[46] J.P. Perdew, J.A. Chevary, S.H. Vosko, K.A. Jackson, M.R. Pederson, D.J. Singh, C. Fiolhais, Physical Review B 46 (1992) 6671–6687.
[47] D. Vanderbilt, Physical Review B 41 (1990) 7892–7895.
[48] W. Gao, M. Zhao, Q. Jiang, ChemPhysChem 9 (2008) 2092–2098.
[49] T.A. Halgren, W.N. Lipscomb, Chemical Physics Letters 49 (1977) 225–232.
[50] R.W.G. Wyckoff, Crystal Structures, 2nd ed., Interscience, New York, 1963.
[51] D.R. Lide, Handbook of Chemistry and Physics, 72th ed., CRC, Boca Raton, FL, 1991.
[52] A. Dianat, N. Seriani, L.C. Ciacchi, W. Pompe, G. Cuniberti, M. Bobeth, Journal of Physical Chemistry C 113 (2009) 21097–21105.
[53] J. Kua, F. Faglioni, W.A. Goddard, Journal of the American Chemical Society 122 (2000) 2309–2321.